AS- Proceedings

3rd International Conference on Scientific and Academic Research

December 25-26, 2023 : Konya, Turkey

ICSAR

AS-Proceedings
https://alls-academy.com/index.php

https://www.icsarconf.com/

The Optical Properties of Sb Doped SnO_2 Thin Film Produced by Spin Coating

Şilan BATURAY[1], Serap YIGIT GEZGIN[2], Hamdi Sukur KILIC[2,3,4]

[1]*Department of Physics, Faculty of Science, Dicle University, 21280 Diyarbakir, Turkey*

[2]*Department of Physics, Faculty of Science, University of Selcuk, 42031 Selcuklu, Konya, Turkey*

[3]*Directorate of High Technology Research and Application Center, University of Selcuk, 42031 Selcuklu, Konya, Turkey*

[4]*Directorate of Laser Induced Proton Therapy Application and Research Center, University of Selçuk, 42031 Konya, Turkey*

Abstract **–** In this study, there is investigated that the optical properties of the 0%, 1%, 2%, and 3% Sb doped SnO_2 thin films produced by spin coating technique. The photon absorption of 3% Sb doped SnO_2 thin film is very high while the non-doped and 2% Sb doped SnO_2 thin films have low absorption and are close to each other. The extinction coefficient of thin films was calculated and its graph was plotted depend wavelength. Refraction indices and dielectric coefficients were calculated and the results interpreted using Herve&Vandamme, Moss and Ravindra relations. The Skin Depth and the optical conductivity characterizes depend band gap of all thin films are drawn and explained.

Keywords –Sb Doped SnO2, Thin Film, Refraction Indices, Skin Depth, Extinction Coefficient

1. Introduction

Tin oxide (SnO_2) thin films, which are transparent conducting materials have found widespread use in gas-sensing performance [1], chemical sensors to H_2S [2], UV-B sensors [3], ozone sensors [4], dilute hydrogen sulfide sensing [5], LPG detection [6], and photoemission detection [7] Tin oxide is one of the best materials for various applications owing to its unique physical features. Because of the favorable features of tin oxide (SnO_2), numerous researchers have studied non-doped and doped SnO2 thin films [8, 9]. In the reports obtained so far, SnO_2 samples formed using different physical and chemical samples deposition techniques; spray deposited [10], sol-gel fabrication process [11], pulsed laser process [12], reactively sputtered [9], and spin coating [13]. Spin coating deposition is the best method for producing tin oxide coated soda lime glass substrates with good optical transmission and low sheet resistance.

SnO_2 is an important semiconducting material with a typical *n*-type direct wide band gap (Eg3.6 eV at 300 K) [14]. It has some interesting properties, including; chemically inert, mechanically durable, and heat resistant [15]. Dopants such as zirconium [13], fluorine [16], cobalt [17], manganese [18], and titanium [19] are used to enhance the electrical, structural and optical characteristics of SnO_2 thin

films. Spin coating process has recently produced low resistivity and high mobility antimony-doped SnO_2 thin film, which exhibits much improved electrical stability than un-doped samples [20]. Gürakar et. al indicated that he optical band gap value, the dielectric constant, and the optical conductivity changes with Sb doping ratio in solution.

There are very few studies in the literature on the characterization of SnO_2 thin films compared to semiconductor thin films such as In_2O_3, ZnO and CuO_2. However, doping significantly changes the structural and surface properties of the SnO_2 thin film. Although there are studies on SnO_2 thin films; there is limited information about the effects on the optical properties of different Sb-doping in SnO_2 thin films obtained using the spin coating process, and Sb-doped SnO_2 samples obtained by the spin coating have not been investigated in detail to date. For this reason, pure and antimony doped SnO_2 films were prepared using spin coating technology in the study. The effects of antimony ions at different concentrations in SnO_2 was detailed discussed. Depending on the various doping concentrations ratio, the optical, characteristics of these films were detailed determined. The optical properties films were evaluated related to the energy band gap, absorbance, the refractive index, the high frequency dielectric constant-(ε_∞) and the static dielectric constant-(ε_o), the Urbach energy, optical conductivity, and skin depth value of the films using UV-Vis spectrophotometer in the 300-1100 nm wavelength at room temperature.

2. Experimental

Fig 1. Systematic illustration of Sb:SnO2 thin film

The pure and antimony doped SnO_2 films were successfully grown on glass substrate using spin coating an aqueous solution of 0.1M tin(II) chloride dehydrate and 0.01 M antimony tricholoride (SbCl3) as sources of tin and antimony ions, respectively. Antimony tricholoride was used for Sb doping with changed concentrations (1, 2, and 3 at% Sb). Glass substrate washing technique is very significant procedure in the manufacture of high quality samples because of the fact that the contamination on the surface of the glass substrate negatively effects quality of the thin film growing and cracking. Therefore, before deposition process, soda lime glass substrates firstly washed with detergent and stirred in ethanol. After obtaining the Sb:SnO_2 solutions and washing process, the films

were then spin coating process at the spin rate of 2000 rpm for 63 s and the acquire solutions were grown on the cleaned substrate for 10 layers of deposition and each layer was heated 220 °C. Having obtained the 10 layers of coating (about 450 nm thickness), all the obtained samples annealed at 450 °C for 1h at a quartz furnace to gain crystal phase in XRD spectra. The conclusion of the energy band gap, absorbance, the refractive index, The high frequency dielectric constant-(ε_∞) and the static dielectric constant-(ε_o), the Urbach energy, optical conductivity, and skin depth value of the films was analyzed using UV-Vis spectrophotometer in the 300-1100 nm wavelength.

3. Optical Properties of the non-doped and Sb:SnO_2 thin films

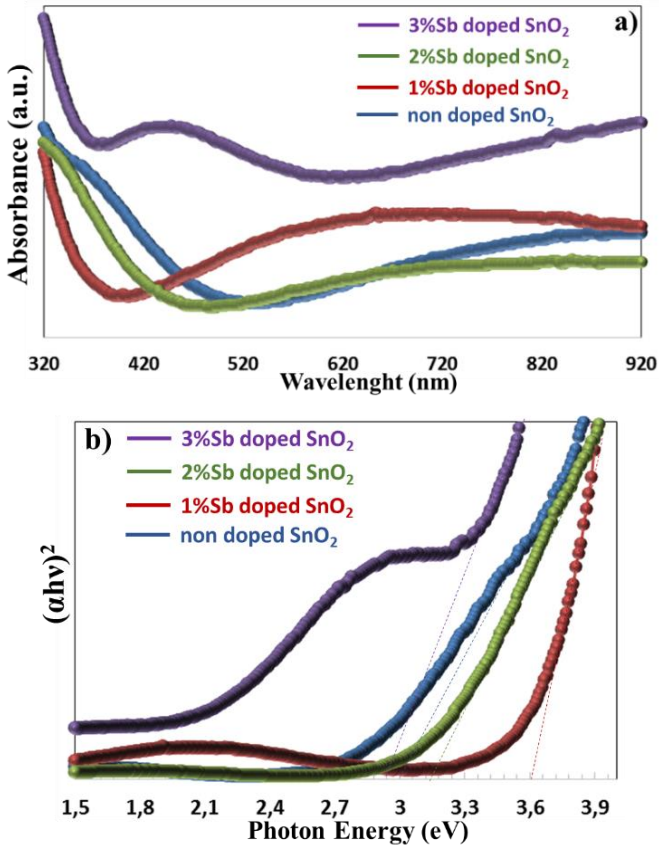

Fig. 2. a) The absorption spectrum and b) the energy band curve of the Sb:SnO_2

In this study, 3% Sb doped SnO_2 thin film absorbs a high amount of photons. The non-doped and 2% Sb doped SnO_2 samples are close to each other and have low photon absorption according to Fig. 2a. 1% Sb doped SnO_2 sample absorbs high photons towards the near infrared region. The non-doped, 2%, and 3% Sb doped SnO_2 samples tend to have low photon absorption in the visible region. The energy band gap graph in Fig. 2b which was obtained using $\alpha h\nu = A\left(h\nu - E_g\right)^{1/2}$ Tauc equation [21]. The band gaps of the 0%, 1%, 2%, and 3% Sb doped SnO_2 samples are 3.00 eV, 3.60 eV, 3.14 eV and 2.90 eV, respectively.

The refractive index of semiconductors used as *n*-type buffer layers in the solar cells that is of great importance in terms of photovoltaic performance.

Three different methods were used in this study to calculate the refractive index safely and accurately. First, the refractive index (n) was calculated using the Moss relations given in Equation (Eq.)1:

$$E_g n^4 = k \quad (1)$$

k is a constant and has a value of 108 eV. The results obtained for all thin films are given in Table 1. Although the refractive indices of thin films are generally low, the lowest refractive index belongs to 1% Sb doped CuO thin film. In order to transmit the light more to the absorbing layer, this refractive indices value is more ideal than other thin films in terms of buffer layer n-type semiconductor.

To verify the refractive indices calculated with Moss relation, the calculations were also made with Herve and Vandamme relation in Eq.(2) [21]:

$$n = \sqrt{1 + \left(\frac{A}{E_g + B}\right)^2} \quad (2)$$

A constant that is 13.6 eV and B constant that is 3.4 eV. The refractive indices calculated with this relation were found to be lower compared to Moss relation. In addition to these two relations, the refractive indices are determined with Ravindra given in Eq. (3) are presented [22] in Table 1.

$$n = 4.16 - 0.85E_g \quad (3)$$

If these three relationships are compared, Moss and Herve&Vandemme relations present results that are closer to each other. Ravindra relation led to the lowest values.

The dielectric coefficient is defined by the electrical field that ensures charge separation and transition in thin films. This charge separation enables significant charge concentration in solar cells. The high frequency dielectric constant-(ε_∞) and the static dielectric constant-(ε_o) which are expressed by Eq. (3) and Eq. (4), respectively[21]:

$$\varepsilon_\infty = n^2 \quad (4)$$

$$\varepsilon_o = 18.52 - 3.08E_g \quad (5)$$

ε_∞ and ε_o values for the non-doped and Sb doped SnO_2 thin films that are given in Table 1. Accordingly, the dielectric coefficients of thin films with low band gap are high. Furthermore, the size of the refractive index of the thin film is a factor that increases the dielectric coefficient. As a result, thin film 3% Sb doped SnO_2 thin film showed the highest the refractive indices and dielectric coefficient, while 1% Sb doped SnO_2 thin film presented the lowest diffraction and dielectric coefficient.

Table 1. Refractive index (n), high frequency dielectric constant (ε_∞) and static dielectric constant (ε_o) of the nondoped and Sb doped SnO_2 thin films

Samples	E_g **(eV)**	**Moss relation**		**Herve&Vandemme**		**Ravindra**		**Static Dielectric Constant,** ε_o
		n	ε_∞	**n**	ε_∞	**n**	ε_∞	
Non-doped SnO_2	3.00	2.44	6.25	2.34	5.47	1.61	2.59	9.28
1%Sb doped SnO_2	3.60	2.34	5.47	2.18	4.75	1.10	1.21	7.43
2%Sb doped SnO_2	3.14	2.42	5.85	2.30	5.29	1.50	2.25	8.84
3%Sb doped SnO_2	2.90	2.47	6.10	2.38	5.66	1.70	2.89	9.58

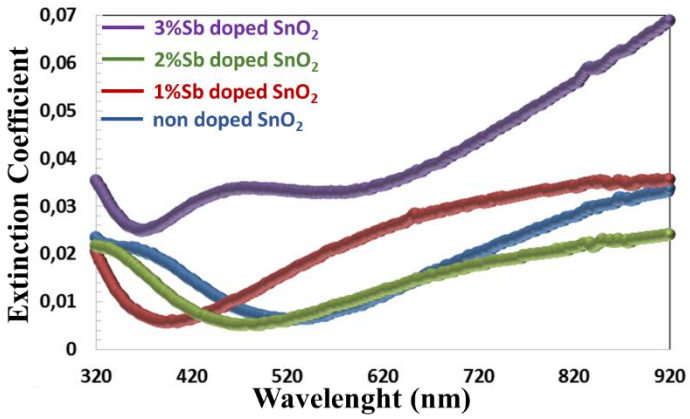

Fig. 3. Extinction coefficient spectra of the non-doped and Sb:SnO_2 thin films

The extinction coefficient is an important parameter for thin films used in solar cells. Light entering the thin film is either absorbed or scattered, depending on particle size, density or defect status. This situation can be defined as the extinction. The extinction coefficient of n-type semiconductors used as buffer layers in solar cells must be low in order to transmit more light. The extinction coefficient (k) is obtained by Eq. (6) [23, 24]:

$$k = \frac{\alpha\lambda}{4\pi} \quad (6)$$

λ is the wavelength number of the light. The absorption coefficient of the thin film is defined as $\alpha = 2.303(A/T)$ [25]. Here, A is the absorbance and T is the thickness of the thin film. According to the wavelength-dependent extinction coefficient spectrum (in Fig. 3) drawn using Eq. (6), while 3% Sb doped SnO_2 thin film shows a high extinction coefficient peak at wavelength 474 nm in the visible region, non-doped SnO_2, 1% Sb, %2 Sb doped SnO_2 thin films exhibit low k values on 539 nm (visible region), 398 nm (ultraviolet region), 477 nm (visible region) wavelength, respectively. All films tend to have high photon absorption in the near-infrared region.

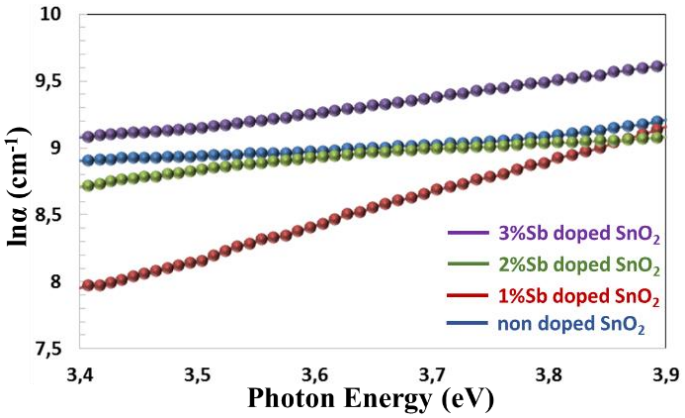

Fig. 4. The Urbach energy of the non-doped and Sb doped SnO_2 thin films

Urbach energy (E_U) describes material disorder as transitions between localized conduction band states and extended valence band states. Eq. (7), as interpreted below, may be used to determine the

disorder in the chemical based on the change in the absorption coefficient.

$\alpha = \alpha_o exp(h\nu/E_U)$

(7)

where α_o is a constant. E_U energy was obtained by slope of $(ln\alpha)$ versus $(h\nu)$ in Fig. 4. E_U values of the non-doped SnO_2, 1% Sb doped SnO_2, 2% Sb doped SnO_2 and 3% Sb doped SnO_2 thin films are 0.75 eV, 2.38 eV, 0.47 eV and 1.21 eV, respectively. Thin films' Urbach energy grow as their band gap decreases. The high Urbach energy value of 1% Sb doped SnO_2 thin film point to more phonon disorder matched to other Sb doped SnO_2 samples. In addition, the high Urbach energy value may be lead to stoichiometric deviation, the distortion in the obtained sample increasing the band tail [26, 27] and localized states density value in the obtained samples [28].

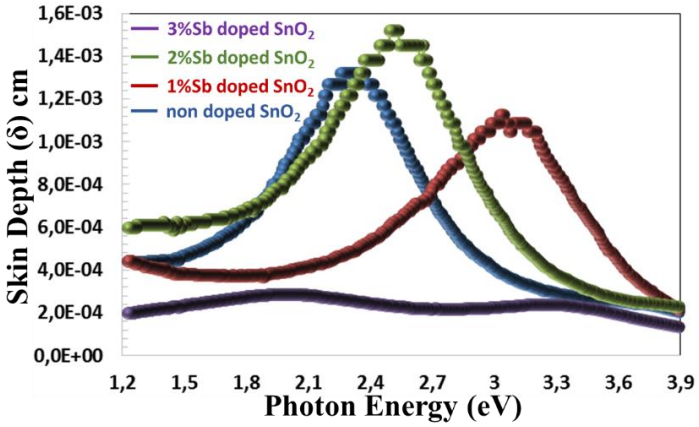

Fig. 5. Skin Depth spectra of the non-doped and Sb:SnO_2 thin films

Depending on the size, shape, number of particles and thickness of the particles that make up the thin film, light incident on the thin film travels to a certain position within the thin film. This distance taken is expressed as Skin depth (χ) [24]. χ parameters of the thin films that is defined by Eq. (8);

$$\chi = \frac{\lambda}{2\pi k} \quad (8)$$

According to Fig. 5, the skin depths of the 0%, 1%, 2%, and 3% Sb doped SnO_2 are 0.0013 cm, 0.0011cm, 0.0015 cm and 0.00028 in 2.25 eV, 3.04 eV, 2.52 eV, 2.00 eV, respectively. The light coming from this band range will be able to diffuse through the thin films and go out easily. In solar cells, this is a good factor so that the light transmission can reach the absorber layer without being restricted.

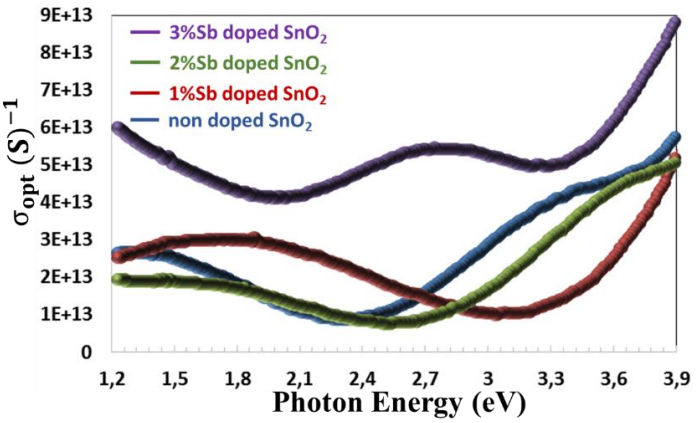

Fig. 6. The optical conductivity ($\sigma_{opt}(S)^{-1}$) spectra of the Urbach energy of the non-doped and Sb doped SnO_2 thin films

The optical conductivity (σ_{opt}) of the non-doped and Sb doped SnO_2 thin films is calculated by Eq. (9);

$$\sigma_{opt} = \frac{\alpha n c}{4\pi} \quad (9)$$

where c is that the light speed. Value of σ_{opt} defines the density of photo excited electrons [26, 29]. (σ_{opt})-photon energy curve of the non-doped and Sb doped SnO_2 thin films that are given as seen in Fig. 6. The highest optical conductivity is presented in 3% Sb doped SnO_2 thin film. However, this feature is more common in *p*-type semiconductors. The lowest optical conductivity was observed in 2% Sb doped SnO_2 thin film. All thin films exhibited optical conductivity compatible with their band gap.

4. Conclusions

In this study, the band gaps of the non-doped SnO_2, 1% Sb doped SnO_2, 2% Sb doped SnO_2 and 3% Sb doped SnO_2 thin films produced by spin coating technique that are 3.00 eV, 3.60 eV, 3.14 eV and 2.90 eV, respectively. The refractive indices calculated with Herve&Vandemme relation were found to be lower compared to Moss relation. Ravindra relation led to the lowest values. thin film 3%Sb doped SnO_2 thin film showed the highest the refractive indices and dielectric coefficient, while 1%Sb doped SnO_2 thin film presented the lowest diffraction and dielectric coefficient. While 3% Sb doped SnO_2 thin film shows a high extinction coefficient peak at wavelength 474 nm in the visible region, non-doped SnO_2, 1% Sb, %2 Sb doped SnO_2 thin films exhibit low k values on 539 nm, 398 nm, 477 nm wavelength, respectively. E_U values of the non-doped SnO_2, 1%Sb doped SnO_2, 2% Sb doped SnO_2 and 3% Sb doped SnO_2 thin films are 0.75 eV, 2.38 eV, 0.47 eV and 1.21 eV, respectively. The highest optical conductivity is presented in 3% Sb doped SnO_2 thin film, while the lowest optical conductivity was observed in 2% Sb doped SnO_2 thin film.

Acknowledgements

Authors would kindly like to thank to

- Selcuk University, Scientific Research Projects (BAP) Coordination Office for the support with the number 21406007, and 22401108 projects,
- Selçuk University, High Technology Research and Application Center (İL-TEK) and
- Dicle University Scientific Research Project (BAP) Coordination for the support with the number FEN.18.007 project,

-

References

1. Brunet, E., et al., Comparison of the gas sensing performance of SnO_2 thin film and SnO_2 nanowire sensors. Sensors and Actuators B: Chemical, 2012. **165**(1): p. 110-118.

2. Vasiliev, R., et al., CuO/SnO_2 thin film heterostructures as chemical sensors to H_2S. Sensors and Actuators B: Chemical, 1998. **50**(3): p. 186-193.

3. Oshima, T., T. Okuno, and S. Fujita, UV-B sensor based on a SnO_2 thin film. Japanese journal of applied physics, 2009. **48**(12R): p. 120207.

4. Korotcenkov, G., et al., Effect of air humidity on gas response of SnO_2 thin film ozone sensors. Sensors and Actuators B: Chemical, 2007. **122**(2): p. 519-526.

5. Tamaki, J., et al., Dilute hydrogen sulfide sensing properties of $CuO–SnO_2$ thin film prepared by low-pressure evaporation method. Sensors and Actuators B: Chemical, 1998. **49**(1-2): p. 121-125.

6. Haridas, D., K. Sreenivas, and V. Gupta, Improved response characteristics of SnO_2 thin film loaded with nanoscale catalysts for LPG detection. Sensors and Actuators B: Chemical, 2008. **133**(1): p. 270-275.

7. Kawabe, T., et al., Photoemission study of dissociatively adsorbed methane on a pre-oxidized SnO_2 thin film. Surface science, 2000. **448**(2-3): p. 101-107.

8. Haridas, D. and V. Gupta, Enhanced response characteristics of SnO_2 thin film based sensors loaded with Pd clusters for methane detection. Sensors and Actuators B: Chemical, 2012. **166**: p. 156-164.

9. Montero, J., J. Herrero, and C. Guillén, Preparation of reactively sputtered Sb-doped SnO_2 thin films: Structural, electrical and optical properties. Solar Energy Materials and Solar Cells, 2010. **94**(3): p. 612-616.

10. Thangaraju, B., Structural and electrical studies on highly conducting spray deposited fluorine and antimony doped SnO_2 thin films from $SnCl_2$ precursor. Thin solid films, 2002. **402**(1-2): p. 71-78.

11. Benrabah, B., et al., Impedance studies of Sb doped SnO_2 thin film prepared by sol gel process. Superlattices and Microstructures, 2011. **50**(6): p. 591-600.

12. Kim, H., R. Auyeung, and A. Piqué, Transparent conducting F-doped SnO_2thin films grown by pulsed laser deposition. Thin solid films, 2008. **516**(15): p. 5052-5056.

13. Zhang, X., et al., Characterization studies of the structure and properties of Zr-doped SnO_2 thin films by spin-coating technique. Superlattices and Microstructures, 2018. **123**: p. 330-337.

14. Muliyadi, L., et al., Synthesis of SnO_2 Thin Layer with a Doping Fluorine by Sol-Gel Spin Coating Method. Jurnal Penelitian Pendidikan IPA, 2019. **5**(2): p. 175-178.

15. Drabeski, R.G., et al., Raman and photoacoustic spectroscopies of SnO_2thin films deposited by spin coating technique. Vibrational Spectroscopy, 2020. **109**: p. 103094.

16. Susilawati, et al. Characteristics and Optical Properties of Fluorine Doped SnO_2 Thin Film Prepared by a Sol–Gel Spin Coating. in Journal of Physics: Conference Series. 2019. IOP Publishing.

17. Soumya, S. and T. Xavier, Effect of cobalt doping on the microstructural, optical and electrical properties of SnO_2 thin films by sol-gel spin coating technique. Physica B: Condensed Matter, 2022. **624**: p. 413432.

18. Xiao, Y., et al., Room temperature ferromagnetism of Mn-doped SnO_2 thin films fabricated by sol–gel method. Applied Surface Science, 2008. **254**(22): p. 7459-7463.

19. Sivakumar, P., et al., Effect of Ti doping on structural, optical and electrical properties of SnO_2transparent conducting thin films deposited by sol-gel spin coating. Optical Materials, 2021. **113**: p. 110845.

20. Liu, S., et al., Effect of Sb doping on the microstructure and optoelectrical properties of Sb-doped SnO_2 films prepared by spin coating. Physica Scripta, 2012. **85**(6): p. 065601.

21. Yiğit Gezgin, S. and H.Ş. Kiliç, The effect of Ag plasmonic nanoparticles on the efficiency of CZTS solar cell: an experimental investigation and numerical modelling. Indian Journal of Physics, 2023. **97**(3): p. 779-796.

22. Ravindra, N., P. Ganapathy, and J. Choi, Energy gap–refractive index relations in semiconductors–An overview. Infrared physics & technology, 2007. **50**(1): p. 21-29.

23. Manifacier, J., et al., Optical and electrical properties of SnO_2 thin films in relation to their stoichiometric deviation and their crystalline structure. Thin solid films, 1977. **41**(2): p. 127-135.

24. Habubi, N., S. Oboudi, and S. Chiad, Study of some optical properties of mixed SnO_2-CuO thin films. 2012.

25. Gezgin, S.Y., Modelling and investigation of the electrical properties of CIGS/n-Si heterojunction solar cells. Optical Materials, 2022. **131**: p. 112738.

26. AlKhalifah, M., I. El Radaf, and M. El-Bana, New window layer of $Cu_2CdSn_3S_8$ for thin film solar cells. Journal of Alloys and Compounds, 2020. **813**: p. 152169.

27. Raj Mohamed, J. and L. Amalraj, Effect of precursor concentration on physical properties of nebulized spray deposited In_2S_3 thin films. Journal of Asian Ceramic Societies, 2016. **4**(3): p. 357-366.

28. Ikhmayies, S.J. and R.N. Ahmad-Bitar, A study of the optical bandgap energy and Urbach tail of spray-deposited CdS: In thin films. Journal of Materials Research and Technology, 2013. **2**(3): p. 221-227.

29. Alsaad, A., et al., Structural, optoelectrical, linear, and nonlinear optical characterizations of dip-synthesized undoped ZnO and group III elements (B, Al, Ga, and In)-doped ZnO thin films. Crystals, 2020. **10**(4): p. 252.